Article

Determination of Relationship between Higher Heating Value and Atomic Ratio of Hydrogen to Carbon in Spent Coffee Grounds by Hydrothermal Carbonization

Jung Eun Park, Gi Bbum Lee [ID]**, Cheol Jin Jeong, Ho Kim and Choong Gon Kim *** [ID]

Center for Bio Resource, Institute for Advanced Engineering, Yongin-si 17180, Korea;
jepark0123@gmail.com (J.E.P.); mnbbv21c@gmail.com (G.B.L.); fejin@iae.re.kr (C.J.J.);
hokim0505@gmail.com (H.K.)
* Correspondence: choonggon@gmail.com

Abstract: This study was a preliminary investigation of solid recovered fuel production from spent coffee grounds using the hydrothermal carbonization (HTC) technique. The spent coffee grounds (SCGs) were subjected to HTC at 170 to 250 °C. The biochar was characterized by proximate analysis, ultimate analysis, capillary suction time, time to filter, suspended solids, and particle size distribution. The biochar yields decreased with increasing HTC temperature and time. However, the higher heating value (HHV) of biochar increased with the HTC temperature and time. The H/C slop relative to the O/C atomic rate of spent coffee grounds was 0.10 with low decarboxylation selectivity. Considering the HHV of biochar and dehydration capacity depend on ratio of H/C vs. O/C, the optimum reaction temperature of HTC was 200 °C, and the biochar from SCGs is an attractive biochar.

Keywords: biochar; energy density; hydrothermal carbonization; proximate analysis; reaction temperature; spent coffee grounds

1. Introduction

The quantity of spent coffee grounds (SCGs) produced has been continuously increasing with the worldwide increase in coffee consumption [1–3]. SCGs is generated during the coffee extraction process, creating various environmental problems [1]. Some are landfilled or incinerated depending on the waste disposal standards [2]. Thus, developing a simple, efficient, low-cost method for solving environmental pollution and converting it into valuable energy products is important.

SCGs are used as a renewable energy resource and can be upgraded by specialized recycling technologies for various purposes such as composting, gardening, and bioenergy production [3]. The organic SCGs waste partially decomposes into methane, contributing to climate change [4]. SCGs contains 10–20% oil, depending on the extraction method, and can be used for bio-fuel production [5,6]. The solid SCGs before or after oil extraction are used as biochar [7,8]. Recently, biochar from biomass with high calorific fractions of non-hazardous waste materials has been produced to EU specifications (European Committee for Standardization, 2011) and is recognized as a viable alternative to fossil fuels [9].

SCGs are used as a source of energy and have become important due to the upgrade provided by thermochemical processes. Before hydrothermal carbonization (HTC) processing, the lignocellulosic biomass presents obstacles to direct combustion, such as high-moisture content, heterogeneous composition, and low energy density.

Therefore, studies on applying thermochemical transformations such as HTC for biochar production have recently been conducted [10]. Thermochemical carbonization has focused on low-temperature hydrothermal processes producing low oxygen-content compounds and upgrading high-moisture materials. Under hydrothermal conditions, the lignocellulosic material is physiochemically converted in the presence of water that serves

as an active transfer medium for ions moving from one bond to another, high solubility, and catalytic functionalities [11,12]. HTC involves reactions such as hydrolysis, dehydration, decarboxylation, aromatization, and recondensation to produce biochar [12,13].

1.   Primary Reaction: Dehydration $4(C_6H_{10}O_5)_n \leftrightarrow 2(C_{12}H_1O_5)_n + 10\ H_2O$
2.   Secondary Reactions: Decarboxylation, Decarboxylation/Decarbonylation

Hydrothermal carbonization has been used to simulate natural coalification in coal petrology for nearly a century, and several published studies have reported on it [14,15]. It is an exothermic process that lowers the oxygen and hydrogen content of the raw materials to be dehydrated and decarboxylated. The HTC process conditions require a water phase that is an appropriate reaction for SCGs [16]. The physicochemical properties of SCGs change with raw material variations, including carbonization temperature, time, pressure, and water precursor ratio. Therefore, the type of biomass precursor affects the energy content.

In this study, HTC was performed on high-moisture-content SCGs, and the effectiveness of the biochar heat generation was evaluated based on temperature and time. Additionally, the heat generation pattern related to oil concentration was analyzed, and a property characteristic evaluation was conducted.

2. Materials and Methods

2.1. Materials

Spent coffee grounds (SCGs) were used as a precursor material for HTC. The moisture content and raw materials properties of SCGs were dependent on the characteristics of raw materials and the methods of recovery. The samples treated by different temperatures such as 170, 200, 220, and 250 °C were denoted as SCG (temperature, time) (for example, SCG(200,1) was 200 °C for 1 h). The biochar was prepared by different reaction times such as 1, 3, and 5 h at 250 °C. It was denoted as SCG(250,1), SCG(250,3), and SCG(250,5).

2.2. Hydrothermal Carbonization (HTC)

The dried SCGs of 300 g and water of 700 g were added to a high-pressure reactor (UTO Engineering, Gyeonggi-do, South Korea) and kept closed under autogenous pressure with constant agitation (Figure 1). The reactor was sealed, and the stirrer was set at 200 rpm with purged N_2 gas for 1 h. HTC temperature was performed over 160 °C, which is the boundary condition of HTC, as shown in Figure S1. Therefore, in this research, HTC temperatures were 170, 200, 220, and 250 °C for 1 h. The reactor-heating procedure was as follows: (1) the contents of the reactor were heated at approximately 5 °C·min^{-1} until the required temperature was reached, (2) the reactor temperature was held constant for residence times, and (3) the reactor stirring was stopped after the residence time when 30 °C was reached. The production was separated from the biochar by vacuum filtration using a filter paper (325 Glass Microfiber filter, Whatman, Maidstone, UK). This analysis required all moisture to be removed from the samples; therefore, they were dried in an oven at 105 °C for 24 h (DF-4S, Daeheung Science, Inchen, South Korea).
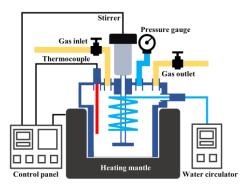

Figure 1. Hydrothermal carbonization reactor scheme.

2.3. Characterization of Biochar

The mass yield was calculated using Equation (1).

$$\text{Equation}: \text{Biochar Yield (\%)} = \frac{\text{Mass of the dry sample}}{\text{Mass of the sample}} \times 100 \qquad (1)$$

The dried samples were placed in a furnace (DF-4S, Daeheung Science, Inchen, South Korea) and heated at 950 °C for 7 min and then at 750 °C for 10 h for proximate analysis. The sample products, including ash, and volatile and fixed carbon content, were measured as percentages of the total weight [16].

Elemental analysis (EA) was performed for 12 min at 900 °C using an elemental analyzer (628 series, LECO, St. Joseph, MI, USA) to determine the C, H, O, N, and S elemental contents [17]. The measured value was measured five times, and the results used the average value.

The materials adsorbed on the activated carbon (AC) were analyzed for ash content using X-ray fluorescence (XRF-1800, Shimadzu, Kyoto, Japan).

For the dehydration evaluation of coffee sequencing samples, the general methods of capillary suction time (CST) and time to filter (TTF) were used.

Capillary suction time (CST) is used to measure sludge filtration; however, it can also identify relative dehydration properties. CST measures the time taken for moisture to travel 1 cm through filter paper (17 CHR, Whatman, Maidstone, UK) after placing approximately 5 mL of the sample into the device. The time to filter (TTF) is a measure of the time it takes for 50% of the target sample volume to escape into the surplus; it was measured more than three times on average, using filter paper (No. 2, Whatman, Maidstone, UK) in a Buchner funnel to measure the time taken for the extra 100 mL of sample to reach 50 mL by forming a negative pressure with a vacuum pump.

Suspended solid (*SS*) is residual particle solids in the filtrate, including organic and inorganic particles. Two grams of dried samples were added to 50 times their weight of distilled water and stirred for more than 12 h to evenly disperse the samples. Thirty-milliliter samples were collected and dried at 105 °C for 24 h, and the *SS* was calculated using Equation (2) with the following formula:

$$\text{Equation}: SS\left(\frac{mg}{L}\right) = \frac{\text{Weight of filtered solid}}{\text{Diluted sample volume}} \times 1,000,000 \qquad (2)$$

The particle size distribution of the samples was measured by laser diffraction using a particle size analyzer (Mastersizer 2000, Malvern Panalytical Ltd., Worcestershire, UK). The sample was injected within a concentration range of 10–20% for measurement. The detector measured the intensity of laser light scattered, and the result was reported on an Equivalent Spherical Diameter Volume basis. For the result values, the average of the measured values repeated 30 times was used.

The image of the SCGs was obtained by scanning electron microscopy (SEM) using an CX-200 (COXEM, Daejeon, South Korea), and the images were obtained by applying an acceleration voltage 20 kV.

The samples were analyzed for natural detergent fiber (NDF), acid detergent fiber (ADF), and acid detergent lignin (ADL) [18]. The NDF, ADF, and ADL contents were determined according to Van Soest et al. (1991) using an ANKOM 220 Fiber Analyzer (ANKOM Technology Corporation, New York, NY, USA). The hemicellulose content was calculated as NDF–ADF and cellulose as ADF–ADL. The higher heating values (HHV) of the samples were evaluated using a Parr 6200 adiabatic oxygen bomb calorimeter (Parr Instrument Company, Moline, IN, USA) calibrated with benzoic acid using standard methods [18]. All samples were prepared by weighing a representative mass (1.0 g) with a 1 mm particle size for uniform heating values.

Dry ash-free HHV (HHV_{daf}) was calculated using Equation (3), and the energy densification (ED) was calculated using Equation (4) to evaluate how the HHV changes in the sample.

$$HHV_{daf} = \frac{HHV \text{ of the sample}}{1 - \text{Faction of dry ash into the sample}} \tag{3}$$

$$\text{Energy Densification (ED)} = \frac{HHV \text{ of the biochar}}{HHV \text{ of the spend coffee grounds (SCGs)}} \tag{4}$$

The adsorbate was extracted with 100 mL of solvent and shaken twice over 5 min. After separation, the extracted adsorbate in n-Hexane was boiled at 80 °C. The adsorbate contents yielded was expressed in terms of the mass percentage of the samples. The extracted adsorbate yield can be estimated using following Equation (5). For the result values, the average of the measured values repeated three times was used.

$$\text{Extracted Adsorbate Yield (wt.\%)} = \frac{mass\ of\ extracted\ adsorbate\ (g)}{mass\ of\ adsorbate\ (g)} \times 100 \tag{5}$$

2.4. Characterization of Py-GC/MS

A pyrolyzer (Py-2020iD, Frontier-Laboratories Ltd., Fukushima, Japan) coupled to Gas Chromatography-Mass Spectrometry (GC-MS, Agilent 7890A/Agilent 5973C inert, Agilent Technology, Santa Clara, CA, USA) was used to identify the thermally degraded compounds from the samples. A total of 1 µL of the sample was loaded into pyrolysis samples cup and free fallen into the preheated furnace at 550 °C under a He atmosphere. The pyrolysis products were transferred to a metal capillary column (UA-5, 30 m × 0.25 mm i.d. × 0.25 µm f.t.). The column temperature was programmed to change from 40 to 320 °C, and the total flow rate was 1.0 mL·min^{-1} and the spilt ratio was 100:1. The peaks were identified using the National Institute of Standards and Technology Mass Spectral Library and Search Program (NIST 08 and Version 2.0f, Gaithersburg, MD, USA).

3. Results and Discussion

3.1. Biomass Properties

The proximate analysis and ultimate analysis of SCGs are shown in Table 1. The moisture content of SCGs was <50%. In the case of biomass (such as cashew nutshell, rice straw, chaff, peanut peel, and sawdust), the moisture contents are approximate under 10% (7.6%, 8.5%, 7.4%, 9.0%, and 9.3%) for HTC [19,20].

Table 1. The proximate analysis and ultimate analysis of spent coffee grounds (SCGs).

Moisture (%)		**55.2 ± 9.0**
	Volatile Matter (%)	83.3 ± 1.2
Proximate analysis—dry basis	Fixed-C (%)	1.5 ± 0.7
	Ash (%)	15.3 ± 1.9
	Sum (%)	100
	Carbon (%)	54.2 ± 0.7
	Hydrogen (%)	7.0 ± 0.2
Ultimate analysis—dry basis	Oxygen (%)	33.1 ± 0.8
	Nitrogen (%)	2.4 ± 0.2
	Sulphur (%)	0.0
	Sum (%)	96.7 ± 0.1

From the proximate results, SCGs were one of the best candidates for HTC due to their high water content despite a low fixed-C. Generally, the moisture required approximately

60% for hydrolysis at HTC. Otherwise, biomasses required the addition of water for the HTC reaction to proceed, which is considered impractical because of increased reactor size and energy loss.

3.2. HTC of SCGs at Different Temperatures

As shown in Table 2 and Figure 2, the biochar yield is directly influenced by the HTC temperature.

Table 2. Proximate and ultimate analysis of Biochar.

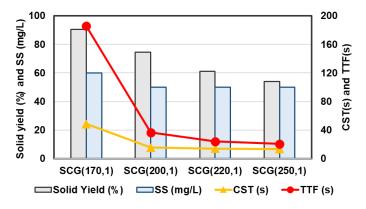| Biochar		SCG(170,1)	SCG(200,1)	SCG(220,1)	SCG(250,1)
Proximate analysis—dry basis	Volatile matter (%)	80.9 ± 1.8	79.1 ± 1.6	75.2 ± 1.4	62.8 ± 1.5
	Fixed-C (%)	17.9 ± 1.6	19.7 ± 1.4	23.8 ± 1.1	36.2 ± 1.0
	Ash (%)	1.2 ± 0.4	1.2 ± 0.3	1.0 ± 0.3	1.0 ± 0.3
	Sum (%)	100.0	100.0	100.0	100.0
Ultimate analysis—dry basis	Carbon (%)	53.1 ± 0.4	54.2 ± 1.1	66.2 ± 1.2	68.7 ± 1.6
	Hydrogen (%)	7.5 ± 0.4	6.7 ± 0.8	6.9 ± 0.7	6.3 ± 0.5
	Oxygen (%)	31.8 ± 2.1	27.8 ± 1.0	21.9 ± 2.0	16.2 ± 2.6
	Nitrogen (%)	1.7 ± 0.6	2.4 ± 0.7	2.9 ± 0.4	3.2 ± 0.3
	Sulphur (%)	0.0	0.0	0.0	0.0
	Sum (%)	94.1 ± 1.6	91.1 ± 1.0	97.9 ± 1.2	94.4 ± 1.1

Figure 2. Solid yield (%), *SS* (mg/L), CST (s), and TTF (s) depend on SCGs.

The mass loss at 200 °C is primarily due to the decomposition of sugar, not to the thermo-degradation of lignocellulosic constituents [20]. The biochar yield decreased with increasing temperature due to the decomposition of hemicellulose and other sugars, which are more sensitive. However, the primary cellulose decomposition was performed at 250 °C, and the secondary biochar decomposition produced bio-oil and bio-gas, decreasing the biochar yield [20,21]. Previous studies have reported that the mass loss at lower temperatures decreased steadily as the reaction temperature increased.

As the reaction temperature increased, the contents of fixed-C increases and volatile matter decreased. The ash slightly decreased from 1.2% to 1.0% with similar compositions analyzed by XRF (Figure S2.)

Capillary suction time (CST) and time to filter (TTF) are associated with the dehydration of products. The results indicated that the HTC temperature increased with increased dehydration capacity, and the dewaterability increased with increasing temperature. Therefore, according to the CST results, the boundary water should be converted to free water as the temperature increases relative to the biochar density. Additionally, the increase in temperature is correlated with the reduction of *SS* in the liquid.

The results of the proximate SCGs analysis are shown in Table 2. The biochar moisture content was reduced due to solid matrix water loss. The HTC temperature promoted a reduction in the volatile matter and ash content of the biochar. It was difficult to show its relationship to the increase or decrease due to the low ash content. However, the ash content is typically reduced by the leaching of the inorganic solid phase during HTC. The fixed carbon content increased with the HTC temperature due to the formation of carbonaceous species related to the biochar structure. This result was related to the quantity of elemental carbon. The quantity of biochar carbon increased with increasing HTC temperature due to carbonization. Therefore, the carbon, hydrogen, and oxygen contents of the product were measured by elemental analysis and are shown in Table 2.

In the case of SCGs, they have a lower carbon content than other biomass, which is also lower among the samples in this study and is relatively lower in value compared to the agricultural residues [22,23].

The hydrogen and oxygen content in the biochar decreased with increasing HTC temperature. The relationship between nitrogen and temperature was not proportional due to the nitrogen-including raw materials.

The lignin, cellulose, and hemicellulose fractions in the unreacted cellulose were estimated at 23.08%, 14.47%, and 24.98%, respectively. As the reaction temperature increased, the cellulose and hemicellulose contents decreased by 1.3% and 2.2%, respectively, at 250 °C, and the lignin content increased by approximately 42%. As the HTC temperature increased, the cellulose and hemicellulos decomposed the most at approximately 250 °C.

Previous studies have reported that the decomposition rate of raw materials increases as the reaction temperature increases [22,23]. In this study, the particle size was measured according to the reaction temperature (Figure 3). In Figure 3, the fraction of < 0.5 mm in biochar increased with HTC temperature decreasing, while the fraction of > 0.5 mm was shown with an opposite trend [24]. The fraction of 0.1–0.5 mm in biochar was increased with the increase HTC temperature. This can be due to that the excessive atomization or decomposition.
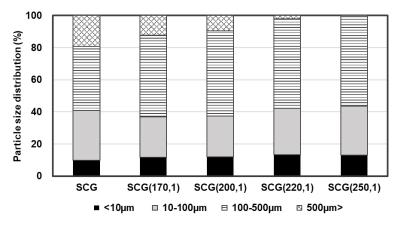

Figure 3. The particles sizes distribution of SCGs at different reaction temperatures.

The scanning electron microscopic (SEM) images of the SCGs revealed the particle size and polydispersity index in Figure S3. Generally, their surface morphology was an irregular shape within the conventional SEM resolution. The overall trend is that as HTC temperature increases, more small particles are shown in Figure S3. This is consistent with the results of particle size distribution in which large particles gradually decrease. The difference is between particle size change and gap of HHV, the optimum temperature required. In conclusion, the optimum HTC temperature is under 220 °C, which is considered the physical properties, boundary of atomization, and HHV.

The Van Krevelen diagram is shown in Figure 4. The plot of H/C versus O/C atomic ratios of the materials provides an estimate of the reaction path. As the reaction temperature increases, it appears that it progresses along the dehydration pathway. The SCGs conducted

in this study were considered to have a relatively low incident of H/C and an O/C atomic ratio of approximately 0.11, consistent with the 0.10 obtained in previous SCGs [25] and coffee beans [26,27]. Additionally, the HTC results using residual coffee materials showed a similar pattern. These slops can be explained in relation to a response selective for decarboxylation and dehydration.
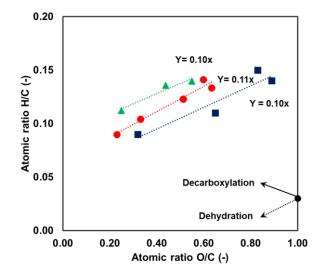

Figure 4. Van Krevelen diagram and classification of materials according to carbon, oxygen, and hydrogen contents. (● SCGs (This study), ▲ SCGs [25], ■ Coffee bean [26,27]).

In previous research, the incident of H/C and O/C of the wood chips, cellulose, leather waste was 1.4 [28], 1.8 [28], and 1.4 [29], respectively. The incidence of the H/C and O/C ratio of the biomass samples showed various gradient values and was higher than that of the coffee materials (Figure S4). It might be that the decarboxylation of SCGs is lower than the other biomass, which is expected to be caused by low fixed carbon.

The slope of the HHV to incident of H/C and O/C showed in Figure 5 is significantly less steep than that of the other biomass samples. The increase in the H/O ratio can be explained by the high dehydration rate. The relationship between SCGs and HHV generally is shown in Figure 5. The SCGs showed the highest HHV among the chemical composition of coffee solids [22].

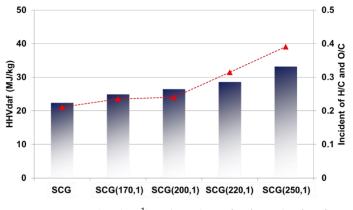**Figure 5.** HHV_{daf} (MJ·kg^{-1}) and incident of H/C and O/C of SCGs.

The incident of H/C and O/C implied the dependence of the reaction on dehydration and decarboxylation. The correlations between the selectivity of a preferential reaction, and HHV can predict the amount of heating generated that could be increased relative to the additional energy that would enter the reaction.

The equation slop of HHV and atomic ratio of H/C and O/C of SCGs was 58.6 ($R^2 = 0.95$). In previous research, the incidence of HHV and atomic ratio of H/C and O/C of SCGs was 27.6 ($R^2 = 0.97$) [25] and coffee bean was 69.3 ($R^2 = 0.90$) [26,27], as shown in Figure S4.

Otherwise, the incident of cellulose and wood chip showed 11.1 ($R^2 = 0.68$) and 11.3 ($R^2 = 0.97$), respectively (Figure S4).

The energy densification factor ranged from 1.00 to 1.47 from HTC and was strongly correlated with the reaction temperature. The correlation between the temperature and energy density ratios is presented in Table 3. In the HTC experiments, the linear regression model appears to fit the data with $R^2 = 0.92 \pm 0.05$.

Table 3. SCGs energy density depend on HTC temperatures.

Samples	SCG	SCG(170,1)	SCG(200,1)	SCG(220,1)	SCG(250,1)
Energy densification (ED)	1.00	1.11	1.18	1.27	1.47
Oil contents in solid (%)	9.9	7.3	5.5	3.4	1.6

The coffee grounds contain oil, and it detected about 9.9% at raw material. The oil content in solid reactants gradually decreases as the reaction temperature increases. Although certain oils are known to help increase HHV, this study determines that they crack by participating in HTC reactions (Figure S4).

3.3. HTC of SCGs at Different Reaction Times

This study was conducted on the HTC reaction time required to produce high-heat-generating biochar [30]. The reaction was conducted under harsh conditions of 250 °C. The results are shown in Table 4.

Table 4. Proximate and ultimate analysis of SCGs (spent coffee grounds) with different reaction times at 250 °C.

Biochar		SCG(250,1)	SCG(250,3)	SCG(250,5)
	Volatile matter (%)	62.8 ± 1.5	61.9 ± 0.9	62.0 ± 1.0
Proximate analysis—dry basis	Fixed-C (%)	36.2 ± 1.0	37.2 ± 1.0	37.9 ± 1.2
	Ash (%)	1.0 ± 0.3	1.0 ± 0.1	0.9 ± 0.2
	Sum (%)	100.0	100.0	100.0
	Carbon (%)	68.7 ± 1.6	67.7 ± 1.8	65.2 ± 1.5
	Hydrogen (%)	6.3 ± 0.5	6.3 ± 0.3	6.7 ± 0.4
Ultimate analysis—dry basis	Oxygen (%)	16.2 ± 2.6	16.2 ± 2.2	18.2 ± 2.0
	Nitrogen (%)	3.2 ± 0.3	0.8 ± 0.6	0.2 ± 0.4
	Sulphur (%)	0.0	0.0	0.0
	Sum (%)	94.4 ± 1.1	91.0 ± 0.9	90.3 ± 1.3

The increase in HTC reaction time showed the same tendency as the reaction temperature. However, the increased rate of fixed carbon over the reaction time was insufficient compared to the energy consumption. Additionally, the HHV of SCGs was similar. In the 3 h reaction, the HHV was 33.66 MJ·kg^{-1}, and the 5 h sample was 33.96 MJ·kg^{-1}, which was approximately like the 1 h samples. From the results, the HTC reaction time was increased with increasing HHV of SCGs, proportionally. However, the insufficient increase in HHV is consistent with the previous results [30].

In particular, the H/O ratio of the 5 h sample was slightly decreased. The main reaction of HTC is dehydration, but decarboxylation and decarboxylation may occur, depending on the reaction conditions. In general, CO_2 from the carboxyl group is emitted at a lower

temperature than CO from carbonyl groups, and the carbonyl group is desorbed at high temperatures [23,30,31]. The decrease in the H/O atomic ratio is affected by carbonylation, consistent with the results of gas emissions from a secondary reaction in which carbonation is performed in the liquid phase.

HTC liquid was analyzed using Py-GC/MS equipment, as shown in Figure 6. As a result, CO_2 peaks were identified in all liquids, and the amount of CO_2 tended to increase slightly as the HTC time increased. As mentioned above, the decarboxylation rate is determined at the reaction temperature and at the reaction time. In addition, phenol was detected at reaction temperatures of 200 and 220 °C at about 8 min, and glycerin was measured at 250 °C from about 6 min. As the higher reaction temperature and the longer reaction time, it detected in more substances the peak, which mean the more likely it is that reactions such as decarboxylation, dehydration, and detention progress in succession (Figure S5).
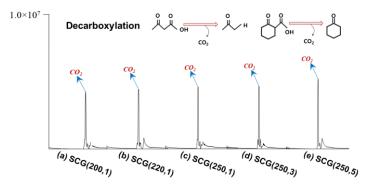

Figure 6. CO_2 peak intensity by Py-GC/MS.

SCGs are very attractive raw materials for biochar despite low fixed-C and recovery. To date, many studies have determined the possibility of biochar using biomass, but its utilization is low. The biochar of HHV of different biomasses is shown in Table 5. Previous HHV studies were compared with the HHV of this study to assess the potential for biochar through HTC, and SCGs were found to have a higher HHV than the other biomass samples, indicating their potential as a valuable fuel source through HTC conversion [32–34]. The producing biochar using SCGs has been carried out in a variety of ways, and as a result, the possibility of biochar is fully demonstrated not only in this research's results but also in previous research. Compared to various biomasses, SCGs have relatively HHV without a process for adding water. Therefore, SCGs are clearly very attractive biomasses.

Table 5. HHV from HTC of different biomasses at 200 °C.

Materials	HHV (MJ/kg)	Ref.
SCG	26.43	This research
Defected Coffee Bean	22.82	[26]
Cellulose	16.19	[28]
Xylan	25.65	[28]
Glucose	23.29	[30]
Cellulose	14.58	[30]
Chitin	16.72	[30]
Chitosan	18.60	[30]
Wood chip	23.12	[30]

4. Conclusions

This study produced and characterized spent coffee grounds (SCGs) for the biochar. A hydrothermal carbonization (HTC) temperature of 170 to 250 °C improved the composition and structure of SCGs with carbonaceous characteristics. The energy density in the synthesized biochar increased with increasing reaction temperature and time. The biochar produced at 250 °C reduced the H/C atomic ratio due to side reactions and particle atomization progresses rapidly. Considering various physical properties and HHV, the biochar produced from SCGs by HTC at 200 °C was the optimum condition, considered a biochar that can replace existing fuels. In addition, the O/C and H/C were caused by decarboxylation and dehydration and the incidence of O/C and H/C was relative to the selectivity of the main reactions. The incident of O/C and H/C of SCGs was 0.10, and it can predict the HHV for further research.

Supplementary Materials: The following are available online at https://www.mdpi.com/article/10.3390/en14206551/s1, Figure S1: Hydrothermal carbonization reaction, Figure S2: X-ray fluorescence results of SCGs, Figure S3: Scanning Electron Microscopes of SCGs, Figure S4: The incident of HHV and the atomic ratio H/C and O/C, Figure S5: Gas Chromatography-Mass Spectrometry of liquid phase depends on SCGs.

Author Contributions: Conceptualization, formal analysis, data curation, G.B.L., C.J.J., H.K.; methodology, validation, data curation, formal analysis, G.B.L. and J.E.P.; writing—original draft preparation, writing—review and editing, J.E.P.; supervision, project administration, funding acquisition, C.G.K., H.K. All authors have read and agreed to the published version of the manuscript.

Institutional Review Board Statement: Not applicable.

Informed Consent Statement: Not applicable.

Data Availability Statement: MDPI Research Data Policies.

Conflicts of Interest: The authors declare no conflict of interest.

References

1. McNutt, J.; He, Q. Spent Coffee grounds: A review on current utilization. *Ind. Eng. Chem.* **2019**, *71*, 78–88. [CrossRef]
2. Saberian, M.; Li, J.; Donnoli, A.; Bonderenko, E.; Oliva, P.; Gill, B.; Lockrey, S.; Siddique, R. Recycling of spent coffee grounds in construction materials: A review. *J. Clean. Prod.* **2021**, *289*, 125837. [CrossRef]
3. Yun, B.Y.; Cho, H.M.; Kim, Y.U.; Lee, S.C.; Berardic, U.; Kim, S. Circular reutilization of coffee waste for sound absorbing panels: A perspective on material recycling. *Environ. Res.* **2020**, *184*, 109281. [CrossRef]
4. Codignole, L.F.; Volpe, M.; Fiori, L.; Manni, A.; Cordiner, S.; Mulone, V.; Rocco, V. Spent coffee enhanced biomethane potential via an integrated hydrothermal carbonization-anaerobic digestion process. *Bioresour. Technol.* **2018**, *256*, 102–109. [CrossRef]
5. Neves, L.; Oliveira, R.; Alves, M.M. Anaerobic co-digestion of coffee waste and sewage sludge. *Waste Manag.* **2006**, *26*, 176–181. [CrossRef] [PubMed]
6. Vardon, D.R.; Moser, B.R.; Zheng, W.; Witkin, K.; Evangelista, R.L.; Strathmann, T.J.; Rajagopalan, K.; Sharma, B.K. Complete utilization of spent coffee grounds to produce biodiesel, bio-oil, and biochar. *ACS Sustain. Chem. Eng.* **2013**, *1*, 1286–1294. [CrossRef]
7. Afolabi, O.O.D.; Sohail, M.; Cheng, Y.-L. Optimisation and characterization of hydrochar production from spent coffee grounds by hydrothermal carbonisation. *Renew. Energy* **2020**, *147*, 1380–1391. [CrossRef]
8. Kim, D.; Lee, K.; Bae, D.; Park, K.Y. Characterizations of biochar from hydrothermal carbonization of exhausted coffee residue. *J. Mater. Cycles Waste Manag.* **2017**, *19*, 1036–1043. [CrossRef]
9. Montanarella, L.; Lugato, E. The Application of Biochar in the EU: Challenges and Opportunities. *Agronomy* **2013**, *3*, 462–473. [CrossRef]
10. Khan, T.A.; Saud, A.S.; Jamari, S.S.; Rahimb, M.H.; Park, J.-W.; Kim, H.-J. Hydrothermal carbonization of lignocellulosic biomass for carbon rich material preparation: A review. *Biomass Bioenergy* **2019**, *130*, 105384. [CrossRef]
11. Funke, A.; Ziegler, F. Hydrothermal carbonization of biomass: A summary and discussion of chemical mechanisms for process engineering. *Biofuels Bioprod. Bioref.* **2010**, *4*, 160–177. [CrossRef]
12. Lucian, M.; Volpe, M.; Fiori, L. Hydrothermal Carbonization Kinetics of Lignocellulosic Agro-Wastes: Experimental Data and Modeling. *Energies* **2019**, *12*, 516. [CrossRef]

13. Zhuang, X.; Zhan, H.; Song, Y.; He, C.; Huang, Y.; Yin, X. Insights into the evolution of chemical structures in lignocellulose and non lignocellulose biowastes during hydrothermal carbonization (HTC). *Fuel* **2019**, *236*, 960–974. [CrossRef]

14. Battista, F.; Barampouti, E.M.; Mai, S.; Bolzonella, D.; Malamis, D.; Moustakas, K.; Loizidou, M. Added-value molecules recovery and biofuels production from spent coffee grounds. *Renew. Sustain. Energy Rev.* **2020**, *131*, 110007. [CrossRef]

15. Nazari, L.; Yuan, Z.; Ray, M.B.; Xu, C. Co-conversion of waste activated sludge and sawdust through hydrothermal liquefaction: Optimization of reaction parameters using response surface methodology. *Appl. Energy* **2017**, *203*, 1–10. [CrossRef]

16. Lee, G.B.; Park, J.E.; Hwang, S.Y.; Kim, J.H.; Kim, S.; Kim, H.; Hong, B.U. Comparison of by-product gas composition by activations of activated carbon. *Carbon Lett.* **2019**, *29*, 263–272. [CrossRef]

17. Suárez, L.; Benavente-Ferraces, I.; Plaza, C.; Pascual-Teresac, S.; Suárez-Ruiza, I.; Centeno, T.A. Hydrothermal carbonization as a sustainable strategy for integral valorisation of apple waste. *Bioresour. Technol.* **2020**, *309*, 123395. [CrossRef] [PubMed]

18. Jančik, F.; Homolka, P.; Čermak, B.; Lad, F. Determination of indigestible neutral detergent fibre contents of grasses and its prediction from chemical composition. *Czech J. Anim. Sci.* **2008**, *53*, 128–135. [CrossRef]

19. Kabakcı, S.B.; Baran, S.S. Hydrothermal carbonization of various lignocellulosics: Fuel characteristics of hydrochars and surface characteristics of activated hydrochars. *Waste Manag.* **2019**, *100*, 259–268. [CrossRef]

20. Yang, L.; He, Q.S.; Havard, P.; Corscadden, K.; Xu, C.C.; Wang, X. Co-liquefaction of spent coffee grounds and lignocellulosic feedstocks. *Bioresour. Technol.* **2017**, *237*, 108–121. [CrossRef]

21. Jenkins, R.W.; Ellis, E.H.; Lewis, E.J.; Paterson, M.; Le, C.D.; Ting, V.P.; Chuck, C.J. Production of Biodiesel from Vietnamese Waste Coffee Beans: Biofuel Yield, Saturation and Stability are All Elevated Compared with Conventional Coffee Biodiesel. *Waste Biomass Valor.* **2017**, *8*, 1237–1245. [CrossRef]

22. Khan, N.; Mohan, S.; Din, P. Regimes of hydrochar yield from hydrothermal degradation of various lignocellulosic biomass. *J. Clean. Prod.* **2021**, *288*, 125629. [CrossRef]

23. Yahya, M.A.; Al-Qodah, Z.; Zanariah Ngah, C.W. Agricultural bio-waste materials as potential sustainable precursors used for activated carbon production: A review. *Renew. Sustain. Energy Rev.* **2015**, *46*, 218–235. [CrossRef]

24. Li, H.; Wang, S.; Yuan, X.; Xi, Y.; Huang, Z.; Tan, M.; Li, C. The effects of temperature and color value on hydrochars' properties in hydrothermal carbonization. *Bioresour. Technol.* **2018**, *249*, 574–581. [CrossRef]

25. Sermyagina, E.; Mendoza, C.; Deviatkin, I. Effect of hydrothermal carbonization and torrefaction on spent coffee grounds. *Agron. Res.* **2021**, *19*, 1. [CrossRef]

26. Santana, M.S. Rafael Alves Pereira, Willian Miguel da Silva Borges, Elton Francisquini, Mário César Guerreiro, Hydrochar production from defective coffee beans by hydrothermal carbonization. *Bioresour. Technol.* **2020**, *300*, 122653. [CrossRef]

27. Martinez, C.L.M.; Saari, J.; Melo, Y.; Cardoso, M.; Almeida, G.M.; Vakkilainen, E. Evaluation of thermochemical routes for the valorization of solid coffee residues to produce biofuels: A Brazilian case. *Renew. Sustain. Energy Rev.* **2021**, *137*, 110585. [CrossRef]

28. Sheng, K.; Zhang, S.; Liu, J.; Shuang, E.; Jin, C.; Xu, Z.; Zhang, X. Hydrothermal carbonization of cellulose and xylan into hydrochars and application on glucose isomerization. *J. Clean. Prod.* **2019**, *237*, 117831. [CrossRef]

29. Lee, J.; Hong, J.; Jang, D.; Park, K.Y. Hydrothermal carbonization of waste from leather processing and feasibility of produced hydrochar as an alternative solid fuel. *J. Environ. Manag.* **2019**, *247*, 115–120. [CrossRef] [PubMed]

30. Simsira, H.; Eltugral, N.; Karagoz, S. Hydrothermal carbonization for the preparation of hydrochars from glucose, cellulose, chitin, chitosan and wood chips via low-temperature and their characterization. *Bioresour. Technol.* **2017**, *246*, 82–87. [CrossRef]

31. Hwang, S.Y.; Lee, G.B.; Kim, H.; Park, J.E. Influence of mixed methods on the surface area and gas products of activated carbon. *Carbon Lett.* **2020**, *30*, 603–611. [CrossRef]

32. Massaya, J.; Chan, K.H.; Mills-Lamptey, B.; Chuck, C.J. Developing a biorefinery from spent coffee grounds using subcritical water and hydrothermal carbonization. *Biomass Convers. Biorefinery* **2021**, in press. [CrossRef]

33. Cervera-Mata, A.; Lara, L.; Fernández-Arteaga, A.; Rufi án-Henares, J.Á.; Delgado, G. Washed hydrochar from spent coffee grounds: A second generation of coffee residues. Evaluation as organic amendment. *Waste Manag.* **2021**, *120*, 322–329. [CrossRef]

34. Schneider, D.; Escala, M.; Supawittayayothin, K.; Tippayawong, N. Characterization of biochar from hydrothermal carbonization of bamboo. *Int. J. Energy Environ.* **2011**, *2*, 647–652.